Received: 31 October 2020 | Revised: 30 May 2021 | Accepted: 31 May 2021

DOI: 10.1002/hyp.14262

WOMEN ADVANCING RESEARCH IN HYDROLOGICAL PROCESSES

WILEY

New snow metrics for a warming world

Anne W. Nolin[1] | Eric A. Sproles[2] | David E. Rupp[3] | Ryan L. Crumley[4] | Mariana J. Webb[1] | Ross T. Palomaki[2] | Eugene Mar[4]

[1]Department of Geography, University of Nevada, Reno, Nevada, USA

[2]Department of Earth Sciences, Montana State University, Bozeman, Montana, USA

[3]Oregon Climate Change Research Institute, College of Earth, Ocean, and Atmospheric Sciences, Oregon State University, Corvallis, Oregon, USA

[4]College of Earth, Ocean, and Atmospheric Sciences, Oregon State University, Corvallis, Oregon, USA

Correspondence
Anne W. Nolin, Department of Geography, University of Nevada, Reno, MS 0154, Reno, NV 89557, USA.
Email: anolin@unr.edu

Funding information
NASA, Grant/Award Number: #NNX16AG35G

Abstract

Snow is Earth's most climatically sensitive land cover type. Traditional snow metrics may not be able to adequately capture the changing nature of snow cover. For example, April 1 snow water equivalent (SWE) has been an effective index for streamflow forecasting, but it cannot express the effects of midwinter melt events, now expected in warming snow climates, nor can we assume that station-based measurements will be representative of snow conditions in future decades. Remote sensing and climate model data provide capacity for a suite of multi-use snow metrics from local to global scales. Such indicators need to be simple enough to "tell the story" of snowpack changes over space and time, but not overly simplistic or overly complicated in their interpretation. We describe a suite of spatially explicit, multi-temporal snow metrics based on global satellite data from NASA's Moderate Resolution Imaging Spectroradiometer (MODIS) and downscaled climate model output for the U.S. We describe and provide examples for Snow Cover Frequency (SCF), Snow Disappearance Date (SDD), At-Risk Snow (ARS), and Frequency of a Warm Winter (FWW). Using these retrospective and prospective snow metrics, we assess the current and future snow-related conditions in three hydroclimatically different U.S. watersheds: the Truckee, Colorado Headwaters, and Upper Connecticut. In the two western U.S. watersheds, SCF and SDD show greater sensitivity to annual differences in snow cover compared with data from the ground-based Snow Telemetry (SNOTEL) network. The eastern U.S. watershed does not have a ground-based network of data, so these MODIS-derived metrics provide uniquely valuable snow information. The ARS and FWW metrics show that the Truckee Watershed is highly vulnerable to conversion from snowfall to rainfall (ARS) and midwinter melt events (FWW) throughout the seasonal snow zone. In comparison, the Colorado Headwaters and Upper Connecticut Watersheds are colder and much less vulnerable through mid- and late-century.

KEYWORDS
climate change, climate model, remote sensing, SNOTEL, snow cover, SnowCloudMetrics

Eugene Mar. Retired.

1 | INTRODUCTION

Snow cover variability affects multiple sectors, from water, energy, and forest management to transportation planning to outdoor recreation and tourism. Historically, snow monitoring has mainly focused on ground-based measurements, with airborne and satellite remote sensing adding more capacity in the past several decades. While ground-based monitoring networks remain valuable, they do not have the spatial coverage, representative geospatial characterization, and predictive capabilities needed by researchers and water managers today. Snow cover products derived from remote sensing require technical expertise and computing resources to produce and interpret, thereby limiting their broader usefulness (Sproles et al., 2018). Gridded snow data from sources such as the Snow Data Assimilation System (SNODAS; National Operational Hydrologic Remote Sensing Center, 2004) and the University of Arizona snow water equivalent product (UA SWE; Broxton, et al., 2019) provide coverage across the conterminous United States are U.S. only and are limited to present-day snow, not future snow. Here, we present a suite of snow metrics that can serve as key climate indicators to support the goals and needs of snow hydrologists, water managers, climate researchers, and various stakeholder groups.

The objectives of this research are to:

1. Produce a new suite of snow metrics for assessing past and future changes in snow cover and snowpacks;
2. Provide web-based visualization tools to communicate these snow metrics;
3. Assess the use of these snow metrics for a small set of varied watersheds for years with low, average, and high snowfall.

This suite of snow metrics was created to address sector concerns and stakeholder questions such as: Where and how have the extent/duration/timing of snow cover changed in the past, and how might it change in the future? How might snowpack storage change over the next several decades in a particular watershed? What has been the climatological frequency of warm winters for vulnerable economic sectors such as ski areas? How might the frequency of warm winters change in mid-century and late-century?

While there have been a number of previously developed snow metrics, to date there have not been spatially extensive metrics that allow users to look at recent and potential future changes in snow cover. Access to these metrics is particularly important for sectors that may not have technical experience with gridded remote sensing and climate data. Thus, we have created and made readily available a suite of metrics including Snow Cover Frequency (SCF), Snow Disappearance Date (SDD), At-Risk Snow (ARS) and Frequency of a Warm Winter (FWW). This suite of metrics aims to provide information to a wide range of researchers and stakeholders, including hydrologists, climatologists, water and land managers, snow sports enthusiasts, climate adaptation planners, and others for whom snow plays a role in decision making.

2 | PREVIOUSLY DEVELOPED SNOW METRICS AND THEIR LIMITATIONS

2.1 | April 1 snow water equivalent

To date, most metrics used to describe changing snowpacks have been limited in their spatial extent and not specifically designed to capture the changing nature of snow cover. The National Resources Conservation Service (NRCS) measures snow water equivalent (SWE) along snow courses (survey transects) monthly and at automated SNOw TELemetry (SNOTEL) stations daily across the western United States. SWE is the amount of water stored in the snowpack (Serreze et al., 1999). Daily SWE and meteorological data from these NRCS sites are used for seasonal streamflow forecasts using regression-based relationships developed for individual watersheds (Garen, 1992).

Although snow course and SNOTEL data were not intended as climate indicators, the data have been available for decades allowing researchers to incorporate SWE measurements into climate research. Since the early part of the last century, snow surveyors and water supply forecasters have used April 1st as the average date of maximum SWE (Church, 1935; McCabe & Legates, 1995), though this varies depending on geographic location and winter temperatures (Serreze et al., 1999). As winter temperatures continue to warm, April 1 SWE may no longer effectively separate accumulation from ablation periods, especially as mid-winter melt events become more common in the maritime snowpacks of Washington, Oregon, and California (Cooper et al., 2016; Knowles, 2015; Mote, 2003; Mote et al., 2018; Sproles et al., 2013, 2017). Depending on climate modes (e.g., El Niño/La Niña, Pacific Decadal Oscillation, etc.) and station elevation, maximum SWE can occur prior to April 1, thereby introducing a bias to watershed budget calculations (Montoya et al., 2014). Seasonal drought outlooks that use April 1 SWE as a climate indicator may miss key precipitation processes leading up to that date. For instance, anomalously low winter precipitation, called a "dry snow drought" (Harpold et al., 2017), is due to the natural variability of synoptic-scale atmospheric circulation and has regional impacts across all elevations. This is important for continental mountain regions where a shift in the storm track can lead to early and mid-winter dry conditions and low SWE. In contrast, warmer than average winter temperatures that lead to a shift from snowfall to rainfall is termed a "warm snow drought" (Harpold et al., 2017) and may be caused by overall increases in winter storm temperatures. Warm snow droughts are most pronounced at low elevations and in maritime snow regions such as the Oregon and Washington Cascades and the California Sierra Nevada, where storm temperatures are close to the melting point (Hu & Nolin, 2020).

The spatial representativeness of SNOTEL and snow course sites is a concern when used for purposes outside of streamflow forecasting. For logistical reasons, in some watersheds snow course and SNOTEL sites may occupy a relatively limited elevation range; thus, high elevation snow and rain-snow transition zones are undersampled (Gleason et al., 2017; Molotch & Bales, 2006; Nolin, 2012). Even with over 800 measurement sites across the western United

States (NRCS https://www.wcc.nrcs.usda.gov/about/mon_automate.html), the monitoring network is sparse, with many larger watersheds having few or no sites. Eastern U.S. watersheds have no SNOTEL or similar ground-based monitoring sites. Moreover, as the climate continues to warm, these sites, most of which were installed in the early 1980s, may become non-representative of watershed-scale SWE (Gleason et al., 2017). This is because snowline elevation in the mountains increases during warm and/or dry winters (Cooper et al., 2016; Sproles et al., 2017). As such, these sites may underestimate trends in snow cover and changes in interannual variability across the seasonal snow zone.

2.2 | Snow cover extent, absence and persistence

Since the earliest years of satellite remote sensing, researchers have mapped snow cover as a way to examine hemispheric climatological patterns (Dewey, 1987; Frei et al., 1999; Matson et al., 1986; Xiao et al., 2004). Metrics such as snow cover extent, SCE (Brown & Robinson, 2011), snow cover absence, SA (Wayand et al., 2018), snow persistence, SP, and snow season, SS (Hammond et al., 2018a, 2018b) have been used to explore multi-decadal, regional and hemispherical snow cover trends ((Brown & Mote, 2009; Brown & Robinson, 2011; Rupp et al., 2013), fine spatial scale patterns relating to wind and avalanche redistribution in mountainous areas (Wayand et al., 2018), and hydrologically-relevant snow persistence and snow season length at the watershed scale (Hammond et al., 2018b). There is a trade-off however, between temporal and spatial resolution satellite data. Finer spatial scale data, such as from Landsat 8, have a 16-day revisit time so even with two satellites there are long gaps in coverage. Such gaps can miss important events such as snowfall and snowmelt events.

2.3 | Snow disappearance date

Another snow metric is the SDD. The presence or absence of snow affects landscape albedo, which in turn controls the energy balance. In snowy climates, SDD signifies the onset of spring and the start of the growing season. The elevational progression of snow disappearance in spring affects Arctic wildlife, with late spring, low elevation snow having a negative impact on populations of caribou and Dall sheep (Boelman et al., 2019; Mahoney et al., 2018). In the western United States, SDD is associated with wildfire activity (Westerling et al., 2006) in the sense that SDD reflects the end of snowmelt and the onset of seasonal declines in soil moisture and fine fuel moisture content. Lundquist et al. (2013) used SDD in their comparison of forested and open sites and showed that in locations with relatively warmer winters forests lose their snow cover earlier than in open areas.

SDD has been measured using ground-based and remotely-sensed measurements. Using decades of station data across the Arctic, Foster (1989) identified trends in snowmelt date as a possible indicator of anthropogenic pollution or climate change affecting the tundra region. In related work, Foster et al. (1992) used satellite remote sensing and station-based data to map snow cover and snow disappearance for locations in Alaska, Canada, Scandinavia, and Siberia. In the various studies using station data, the way SDD was determined is not always clear. For instance, Foster et al. (1992), in his Arctic tundra studies, defined SDD as the first day of the calendar year when station-based snow depth measurements dropped below 1 in. (2.54 cm). In their 2013 meta-analysis, Lundquist et al. (2013) listed SDD as the first day of the calendar year with no snow as reported from station data (though they did not provide a measurement threshold). Lundquist and Lott (2010) used near-surface soil temperature measurements to detect the presence and absence of snow cover, which is also used to identify the SDD.

Such varied uses and ways of recording SDD indicate both the importance of this snow metric and a need for a spatially consistent approach to its measurement. Station-based data are inherently limited in their spatial representation of SDD, though they are critical for calibrating and validating remote sensing measurements of SDD. Temporal factors affecting SDD are also essential to consider. Transient snowfall events can influence SDD detection and can be important for hydrology and wildlife. The variable nature of spring meteorology means that it is not uncommon for spring melt to be followed by spring snowstorms that can drive the actual SDD to be days or even weeks later.

2.4 | Climatologically-based snow metrics: At-risk snow and frequency of a warm winter

2.4.1 | At-risk snow

First defined by Nolin and Daly (2006), ARS is when snowfall is at risk of turning to rainfall under climate warming conditions. Nolin and Daly used the PRISM 4-km gridded climate data (Daly et al., 2002) and a decision tree approach to classify grid cells as either at-risk or not at-risk, based on monthly mean air temperature for December, January, and February. That study's geographic scope covered only the Pacific Northwest (Washington, Oregon, Idaho, and western Montana), where snowfall is often close to the melting point. Their approach used the 0°C monthly mean temperature threshold to partition between rain and snow. The monthly mean 0°C threshold was selected because, though spatial and temporal differences exist, both thermodynamically and practically, it represents a shift from snowfall and snow accumulation to rainfall and declining snowpacks. Their methodology assumed that locations that might warm to that 0°C monthly mean temperature threshold would be at-risk of converting from snowfall to rainfall. For instance, a grid cell with a climatological mean monthly temperature of -2°C for any one of the core winter months (December–February) was classified as ARS for a $+2$°C warming scenario. This data-driven approach was simple but did not consider possible changes in atmospheric circulation and storm patterns. Moreover, the 4-km resolution was too coarse to address changes at more local scales, especially in mountain regions where a 4-km grid cell can span a wide range of elevations and temperatures.

2.4.2 | Frequency of a warm winter

Nolin and Daly (2006) also developed the FWW metric using the PRISM gridded climate data product and monthly mean temperatures for December, January, and February. FWW is computed as the number of winters out of 30 consecutive winters that meet the "warm winter" criterion. A warm winter is defined as one in which the mean monthly temperature exceeds 0°C for any one of the three core winter months (December–February). Thus, if three winters out of 30 winters are classified as warm in a given grid cell, the FWW is 0.1% or 10%. To demonstrate possible impacts of changes in FWW, Nolin and Daly (2006) tabulated the historical and future FWW values for selected ski areas in the study region. All ski areas in the region showed increases in FWW for incremental temperature increases, but the 4-km resolution introduced uncertainty due to the range of elevations in a grid cell.

3 | DESCRIPTIONS OF THE NEW SNOW METRICS

The suite of snow metrics described below is meant to improve upon and augment previously established snow metrics. We include a pair of satellite-derived metrics, SCF and SDD, in conjunction with climate model-derived metrics, FWW and ARS. We have modified the subsetting capabilities of SCF and SDD from Crumley et al. (2020) and have made considerable updates to FWW and ARS from Nolin and Daly (2006). We refer to them as "new" snow metrics because, together, they represent a new paradigm in access to snow information (Crumley et al., 2020). The snow metrics described in the following section are intended to add value through spatial coverage, future climate characterization, more nuanced interpretation, improved data access, and user-driven flexibility.

3.1 | Snow cover frequency (SCF)

SCF is a global, satellite-derived, gridded product representing the frequency of snow cover in a grid cell. It is computed as the number of days that snow is observed on the land surface divided by the number of valid observations for a specified period. SCF uses the global, 500-m, daily, gridded snow cover product, version 6 from NASA's Moderate Resolution SpectroRadiometer (MODIS/Terra MOD10A1). Because the MOD10A1 product is daily and global, it allows the user to compute SCF anywhere globally for the MODIS period of record (February 2000–present). For analysis periods greater than 30 days, we assume SCF to be the empirical equivalent of probability. In recent work, Crumley et al. (2020) describe a version of this SCF metric for the Northern Hemisphere Water Year (WY, October 1–September 30) for WY 2001–2019. Their SCF snow metric is available as a web-based product (SnowCloudMetrics.app) developed using the Google Earth Engine (GEE) framework. Using the app, users can spatially subset SCF by user-defined polygon, U.S. state boundary or Canadian province, elevation range. For the U.S. only, a user can subset by watershed using the USGS hydrologic unit codes (HUC levels 2–12). Here, we have expanded the utility of this metric by providing code for users to run within GEE (i.e., as a GEE developer). In this case, users can select and compute SCF for any sub-annual set of sequential days within the MOD10A1 record (for 2000-present).

3.2 | Snow disappearance date (SDD, Northern Hemisphere extent)

The SDD is a global, satellite-derived, gridded product that maps the last day of the WY when snow is last detected in a pixel. As with SCF, SDD also uses the global, 500-m, daily, gridded snow cover product from MODIS. Starting on the last day of each WY, the algorithm searches back in the WY for the longest period without snow after a minimum of 5 days of snow cover (accounting for cloudy days). Crumley et al. (2020) computed SDD for WY 2001–2019. Like SCF, SDD has been used in wildlife studies for locations where spring snow disappearance affects the survival of young (Van De Kerk et al., 2018). We anticipate that SDD will have value for mountain regions where SDD has been related to the onset of the wildfire season (Westerling et al., 2006) and where spring vegetation phenology varies with snow cover (Huang et al., 2018; Xie et al., 2020).

At this time, SDD spatial coverage is for the Northern Hemisphere only. However, users can choose to download the SDD code, modify it for the Southern Hemisphere timeframe and run it independently as a GEE developer. The same subsetting options are available for SDD as with SCF.

3.3 | At-risk snow (ARS, conterminous U.S. extent)

While originally developed by Nolin and Daly (2006) using PRISM data with a simple temperature offset, the ARS metric presented here uses statistically downscaled climate model output and as such is more physically realistic than the original ARS. This new version of ARS is computed using the gridded NASA Earth Exchange Downscaled Climate Projections (NEX-DCP30) 30 arcsec (approximately 800-m) dataset (Thrasher et al., 2013), which covers the conterminous United States. We compute mean temperature from their average monthly maximum and minimum temperature data from 33 downscaled climate models and four Representative Concentration Pathways (RCPs) (Meinshausen et al., 2011). The data set includes retrospective model runs covering the historical period from 1950 to 2005, and prospective model runs for 2006 to 2099.

We have produced a fully functional code running on GEE that allows the user to compute ARS for any range of years in the period covered by the NEX-DCP30 downscaled climate data. Users can spatially and temporally subset, visualize, explore, and download the ARS data of interest. A user can filter by RCP, global climate model, spatial extent, and period. They can select from any of four CMIP5 RCPs (RCP2.6, RCP4.5, RCP6.0 and RCP8.5) and from numerous

downscaled (800-m) model output (23 models for RCP2.6; 33 models for RCP4.5; 17 models for RCP6.0; and 31 models for RCP8.5). If desired, users can subset by watershed using the USGS hydrologic unit codes (HUC levels 2–12).

3.4 | Frequency of a warm winter (FWW, conterminous U.S. extent)

As with the ARS metric, FWW uses the monthly maximum and minimum temperature data from NEX-DCP30, computing mean temperature from their average. The definition of FWW is the same as in Nolin and Daly (2006), but as with ARS, we use more physically realistic climate model output rather than the simplistically modified PRISM monthly temperatures. The geographic scope covers the conterminous U.S. at 800-m spatial resolution. The temporal range is 1950–2005 for historic FWW and 2006–2099 for future FWW.

For users to compute FWW, we have produced code that runs on GEE. This allows the user to calculate FWW for any range of years in the period covered by the NEX-DCP30 downscaled climate data. As with ARS, users can spatially and temporally subset, visualize, explore, and download the FWW data of interest. A user can filter by emissions scenario, global climate model, spatial extent, and range of years. As with ARS, users can subset by USGS HUC.

When computing FWW, we recommend that users specify a range of at least 30 years so that the calculated values are the empirical equivalent of a statistical probability. For instance, a user can compare FWW for 1979–2009 (historical) with FWW for 2035–2069 (mid-century) or 2079–2099 (late-century). The 800-m gridded data are sufficiently fine spatial resolution that users can explore projected FWW changes for spatial extent as large as the conterminous United States and as small as a headwater catchment, an urban area, and even along an elevation gradient in a ski area. For example, Table 1 gives FWW values for the selected ski areas across the US. These represent major ski resorts in various mountain regions of the U.S. and snow climates (Sturm et al., 1995) including the maritime snow climate of the Sierra Nevada and Cascades (Squaw Valley, CA; Mt. Bachelor, OR), the continental/Alpine snow climate of the northern and central Rocky Mountains (Big Sky, MT; Vail, CO), and the maritime/taiga snow climate of the northern Appalachian mountains (Killington, VT).

This is a simple example of the use of the FWW metric for non-scientists seeking climate change information at the local-to-regional scale.

4 | WATERSHED APPLICATION OF THE NEW SNOW METRICS

In this section we apply the suite of new snow metrics to three watersheds across different regions of U.S.: the Truckee (CA, NV), the Colorado Headwaters (CO), and the Upper Connecticut (ME, VT, NH) (Figure 1).

4.1 | Description of the study watersheds

The study areas are first- and second-order watersheds with critical downstream water use (Figure 1). In the Western U.S., the Truckee River watershed (12 357 km^2) drains from Lake Tahoe and the surrounding Sierra Nevada Mountains, providing water for municipal and industrial use, energy production, environmental flows, recreation, and agriculture in the downstream high mountain desert which

TABLE 1 Frequency of a Warm Winter for selected ski areas. FWW values were computed based on RCP8.5 and are expressed as a percent for each 30-year period

Location		Elevation (m)	Historical 1970–1999	Mid-century 2035–2064	Late-century 2070–2099
Squaw Valley, CA	base	1890	53.3	96.7	100
	mid-mtn	2316	16.7	86.7	100
	summit	2758	13.3	70	96.7
Mt. Bachelor, OR	base	1737	13.3	53.3	96.7
	mid-mtn	2370	0	10	70
	summit	2763	0	3.3	36.7
Big Sky, MT	base	2286	0	23.3	63.3
	mid-mtn	2682	0	0	56.7
	summit	3403	0	0	26.7
Vail, CO	base	2454	0	3.3	36.7
	mid-mtn	3150	0	0	13.3
	summit	3527	0	0	6.7
Killington, VT	base	355	0	10	66.7
	mid-mtn	1095	0	10	50
	summit	1293	0	3.3	30

receives less than 125 mm of precipitation annually (Sterle et al., 2019). In the Rocky Mountains, the Colorado Headwaters watershed (25 480 km^2) lies directly west of the continental divide and provides much of the meltwater for the Colorado River, which provides water to 27 million people (Painter et al., 2017). Finally, in the Eastern U.S., the Upper Connecticut watershed (16 217 km^2) extends through four states and the Connecticut River itself provides drinking water to 4.8 million New England residents (Kennedy

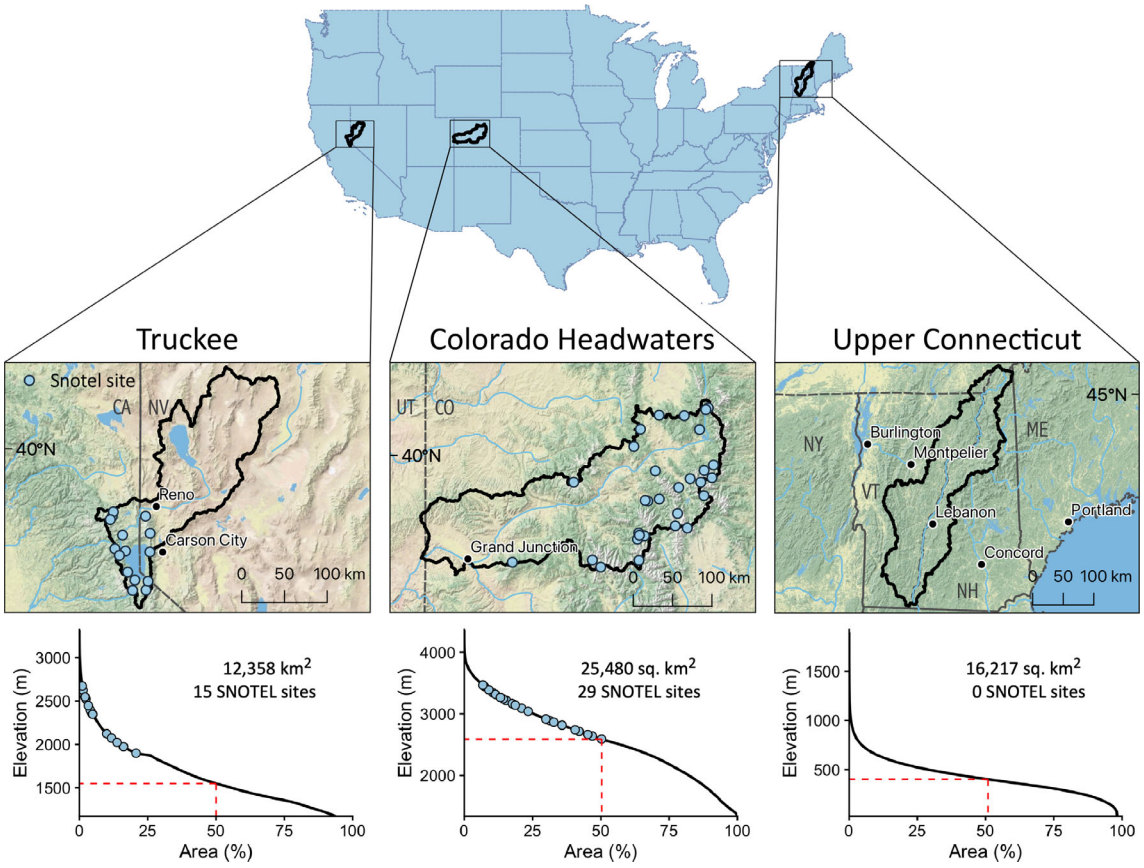

FIGURE 1 Maps and hypsometric relationships for each of the three watersheds used in the new snow metrics examples. Each inset map shows the watershed boundary and location of SNOTEL sites. The plot below each map shows the area-elevation relationship for the watershed with the elevation of each SNOTEL site indicated on the hypsometric curve

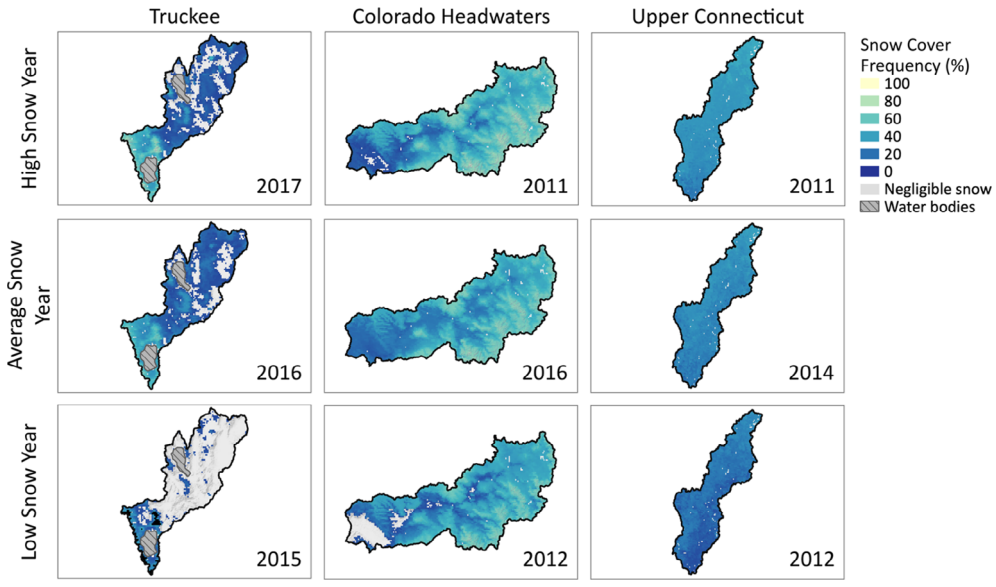

FIGURE 2 Maps of SCF for the three watersheds for high, average, and low snow years

et al., 2018). Although these three watersheds are all located in the U.S., our SCF and SDD can be applied globally. The FWW and ARS metrics use downscaled climate data that are currently available for the U.S. only. However, these could be readily adapted to watersheds outside the U.S. We use these three watersheds for illustrative examples of the new snow metrics.

4.2 | Watershed results for SCF and SDD

Figures 2 and 3 map out SCF and SDD, respectively for each of the three watersheds. We map high, average, and low snow years (watershed-specific), as determined from SNOTEL and regional climate data. The Truckee shows the greatest differences in SCF across the watershed and between 3 years. In the 2015 low snow year, the Truckee had almost no snow in the lower elevations and less than 20% SCF in the seasonal snow zone (historically at elevations >1850 m). The Upper Colorado showed little temporal variability between SCF in the high and average snow years but had negligible SCF at low elevations in the low snow year. The Upper Connecticut shows the least amount of SCF differences spatially and temporally with 40% or less SCF throughout the watershed in the high and average years and 20% SCF or less in the low snow year.

The SDD patterns in Figure 3 resemble the SCF patterns shown in Figure 2. A reasonable explanation is that for these example watersheds and years, higher SCF means higher SWE and therefore later melt-out date. An alternative explanation is simply that higher SCF implies that colder temperatures are controlling snow persistence. Of course, SCF can be controlled by both greater SWE and colder temperatures. The SDD data show that in the temperature-sensitive Truckee watershed, SDD for a low snow year such as 2015 can be as much as 2 months earlier than in a high snow year.

Figure 4 provides an interesting comparison between MODIS-derived SCF and SDD and SNOTEL-derived SCF and SDD. While there is reasonable agreement between MODIS-derived and SNOTEL-derived SCF and SDD, the MODIS-derived metrics show distinct and expected trends in SCF and SDD from low to high snow years, whereas the SNOTEL-derived SCF and SDD are much less sensitive to interannual differences. We attribute the higher sensitivity to the fact that the MODIS-derived SCF and SDD data have a spatial resolution of 500 m and thus encompass a wider range of snow

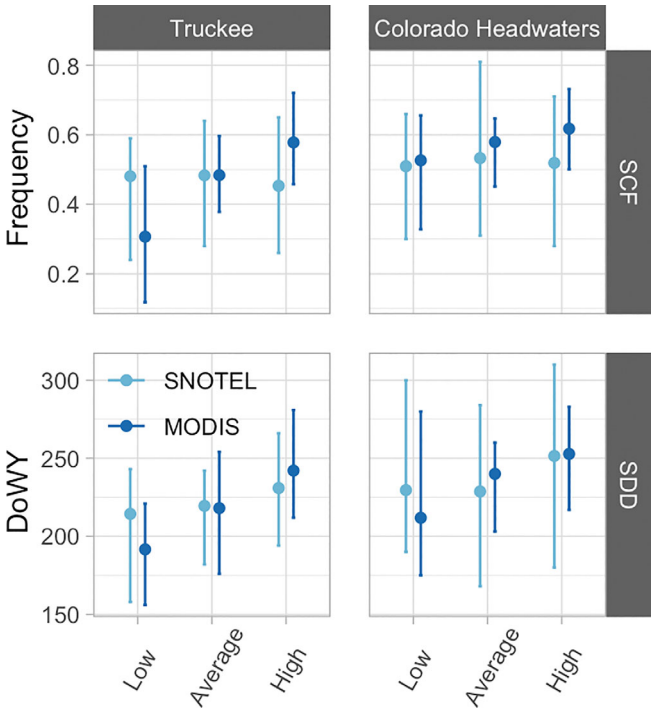

FIGURE 4 Comparison of SNOTEL-derived and MODIS-derived SCF and SDD for the Truckee and Colorado Headwaters watersheds for low, average, and high snow years. For reference, April 1 is the 183rd Day of Water Year (DoWY). The Upper Connecticut is not included in this figure because there are no SNOTEL stations in that watershed

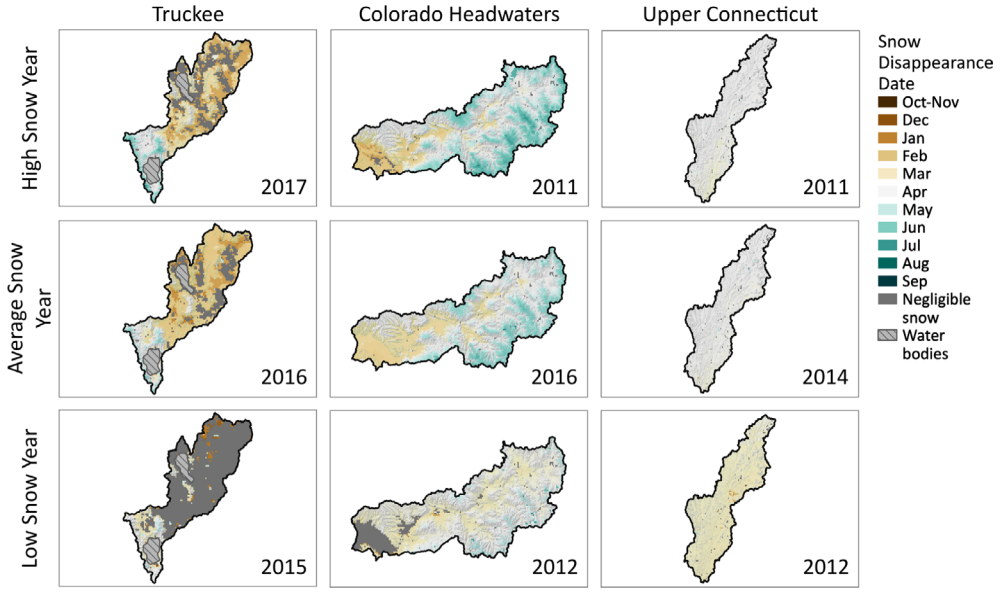

FIGURE 3 Maps of SDD for the three watersheds for high, average, and low snow years

conditions than the point-based SNOTEL station data. The MODIS snow product will not indicate the presence of snow cover if the snow extent in the pixel is less than about 50% (Rittger et al., 2013). Thus, pixels with low/patchy snow cover are likely to be mapped as snow-free. This is not necessarily a concern if the user is aware of the sensitivity of the snow/no snow threshold used in processing the standard MODIS snow product (which can be adjusted in the SCF and SDD snow mapping algorithms, if desired). Another explanation for the lower sensitivity of SNOTEL-derived SCF and SDD is that the SNOTEL sites themselves can act as highly effective snowfall collection sites. SNOTEL sites are open clearings, which are often surrounded by trees and shrubs that act to reduce wind speeds and may increase snow retention compared with the surrounding landscape.

4.3 | Watershed results for FWW and ARS

For illustrative purposes, we present results using the FWW and ARS metrics derived from a single global climate model for each region, though an ensemble approach using multiple models may be preferred when making an assessment of potential climate change impacts (Mote et al., 2011).We chose models that performed better than most with respect to reproducing observed regional climate: ACCESS1.0 in the Sierra Nevada (Lynn et al., 2015), CMCC-CM in the Rocky Mountain West (Bureau of Reclamation, in press) and BCC-CSM1.1 on the East Coast (Karmalkar et al., 2019).

FWW and ARS were calculated using a slightly modified version of the SnowCloudMetrics JavaScript code in GEE (Crumley et al., 2020) to more effectively subset the watershed data. FWW is the empirical probability of the mean monthly temperature in December, January, or February (DJF) exceeding 0°C over a 30-year period (Nolin & Daly, 2006). As mid-winter monthly mean temperatures become more frequent, this suggests that there could be a greater occurrence of mid-winter melt events. ARS is the climatological classification of areas having a mean DJF temperature greater than 0°C over a composite of 30 years. As described in Nolin and Daly, ARS implies that the mid-winter precipitation would likely shift from snowfall to rainfall. Thus, one aspect of this metric is that it might serve as a proxy for mid-winter rain-on-snow events.

From NEX-DCP30 data, we computed FWW and ARS for three, 30-year periods: historic (1970–1999), mid-century (2035–2065), and late-century (2070–2099) and under two RCP scenarios: RCP4.5 and RCP8.5, for a total of six scenarios per watershed. RCP4.5 represents a stabilization of the global rate of greenhouse gas emissions while RCP8.5 assumes increasing greenhouse gas emissions throughout the 21st century (Thomson et al., 2011).

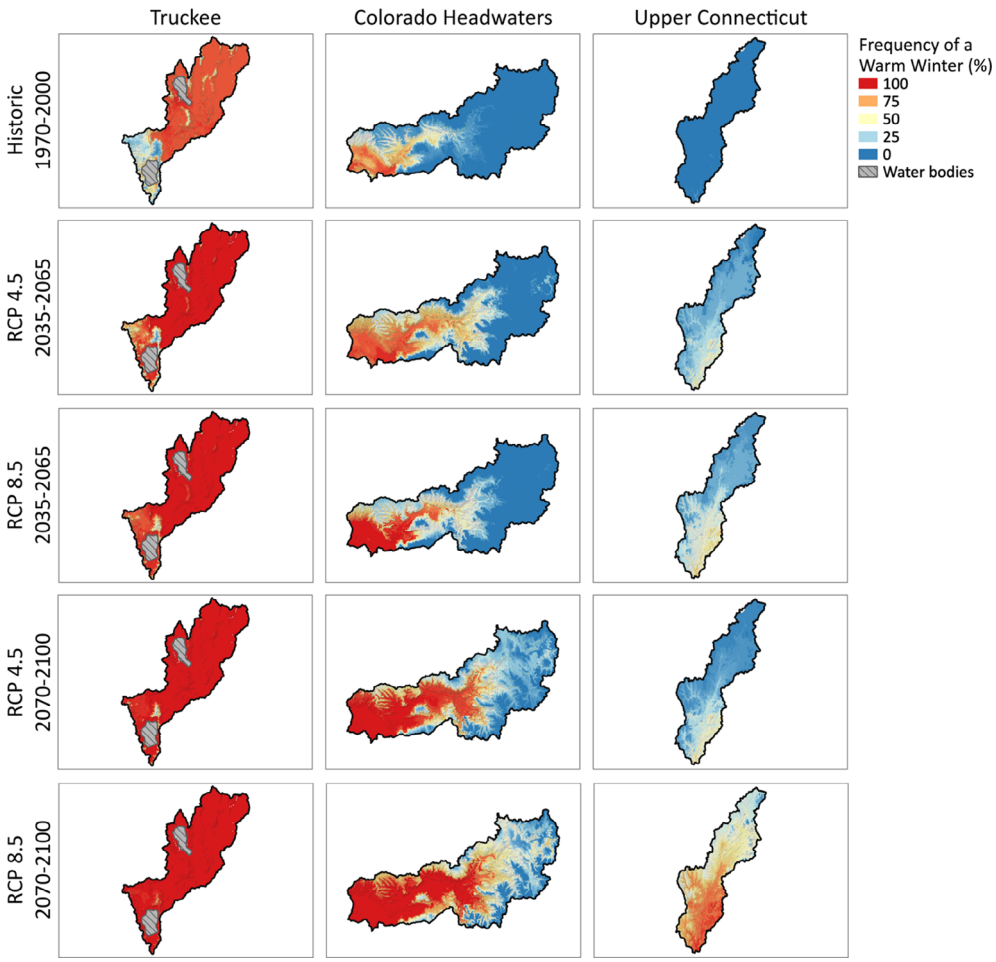

FIGURE 5 Maps of FWW for each of the three watersheds (columns), three time periods, and two climate change scenarios (rows)

We compared climate model-derived FWW and ARS with values computed from SNOTEL temperature data that had been bias-corrected and homogenized (TopoWx; Oyler et al., 2015). The SNOTEL/TopoWx historic period covered the period 1984–2005 (21 years) for which the data were consistently available across all the SNOTEL sites in the Truckee and Colorado Headwaters watersheds. The Truckee watershed has 15 SNOTEL stations while the Colorado Headwaters has 29 SNOTEL stations. Across both watersheds, the SNOTEL sites are primarily located in the upper reaches of the watershed (Figure 1).

The FWW analysis showed distinct patterns and differences between the three watersheds (Figure 5). The Truckee watershed shows a high frequency of warm winters (mean 79%) already occurring in the historic period with little difference between RCP5.5 and RCP8.5 (Figure 5). By late century, the impacts on snow in the Truckee are severe, with a spatially-averaged FWW value of 99%. In the upper part of the Truckee watershed above 1850 m, winter snow plays an important role both hydrologically and economically. This is the area surrounding Lake Tahoe and is home to several ski areas. Focusing on this seasonal snow zone in the Truckee, we observe that, in the historic period only 4% by area of the snow zone is considered at risk and about 12% of the area experiences a high FWW. Here, we define high frequency of a warm winter as FWW > 75%. It is in this seasonal snow zone that major changes are anticipated by mid-century when well over half of the snow zone will be classified as ARS (Figures 6 and 7) and will experience high FWW. By late century, even under the moderate RCP4.5 scenario, 94% of the Truckee snow zone will be experiencing high FWW and 82% of the snow zone will be classified as ARS. For the RCP8.5 late-century projections, nearly 100% of the Truckee watershed will experience 100% FWW, with areas of negligible snow emerging even at elevations above 1850 m. These changes will greatly reduce snowpack water storage and is likely to be economically damaging to the region's snow sports industry (Table 1).

Compared to the Truckee and Upper Connecticut watersheds, the Colorado Headwaters watershed exhibits a steeper elevation gradient of FWW, with lower elevations having FWW values of 80%–100% while FWW values are 0% near the Continental Divide (Figure 5). Interestingly, in the mid-century scenarios in the Colorado Headwaters, the RCP4.5 shows a spatially larger, although less severe, change in FWW (mean 33%) compared to RCP8.5 (mean 28%). By the late-century, more than half of the area in the Colorado Headwaters watershed will be experiencing high FWW even under the RCP4.5 scenario (Figure 7). Similar to the FWW results, ARS in the Colorado Headwaters is concentrated at the lower elevations in the watershed (Figure 6). Differences between ARS for RCP4.5 and RCP8.5 are more

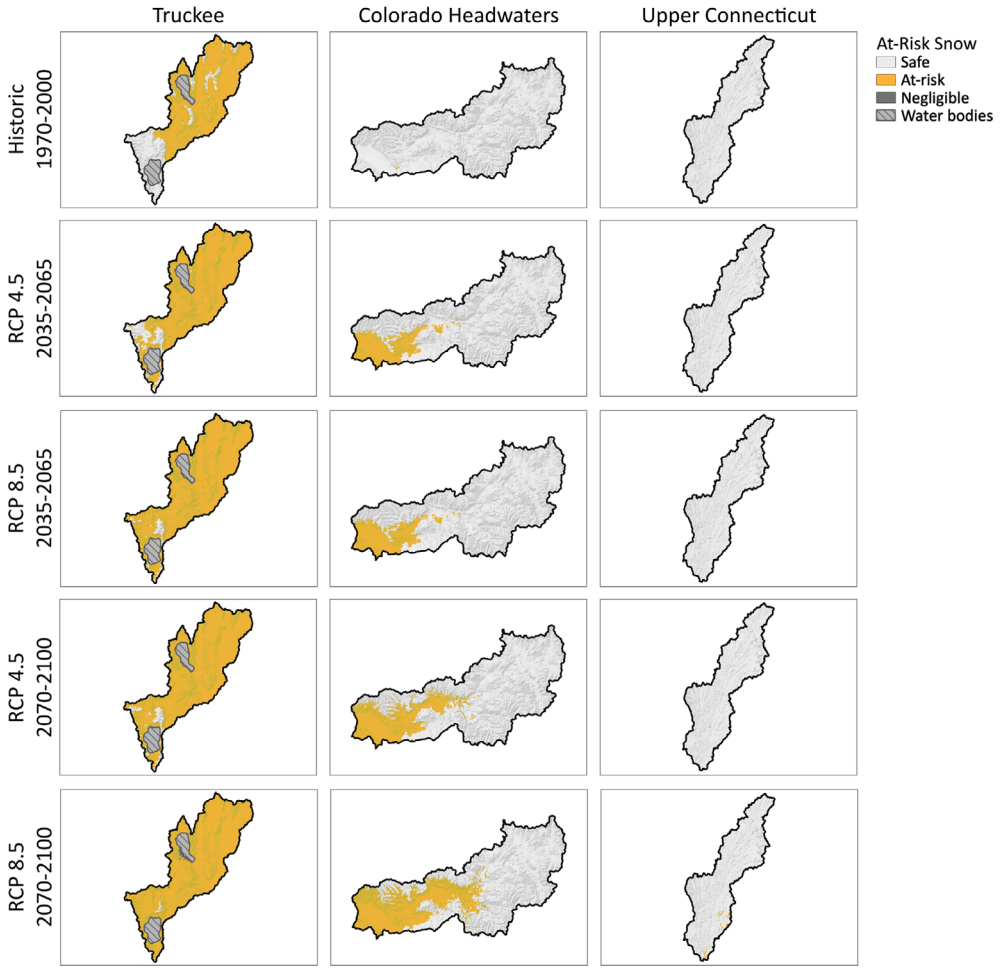

FIGURE 6 Maps of ARS for each of the three watersheds (columns) and for the three time periods and two climate change scenarios (rows)

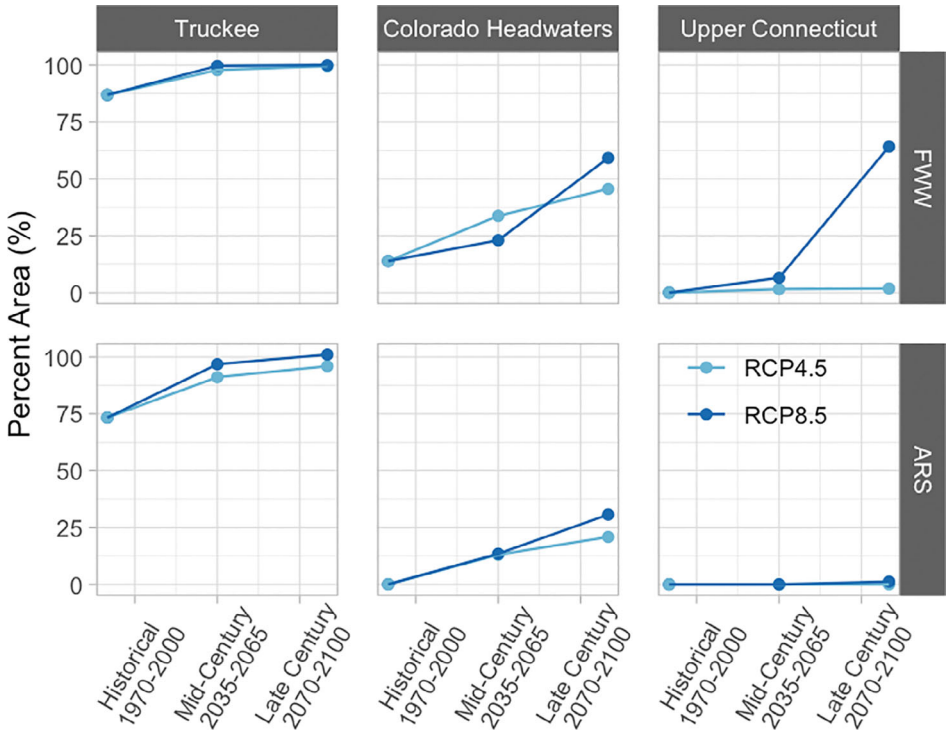

FIGURE 7 Plots of percent area of each watershed have high FWW (>75%) and for ARS for historical, midcentury, and late century time periods, and for RCP4.5 and RCP8.5

subtle for this watershed while differences in ARS are more pronounced between mid-century versus late century. This will reduce snowpack storage, increase winter runoff, and may have significant consequences for both the local economy, which is heavily dependent on winter recreation, and for the downstream users of the Colorado River.

Finally, the Upper Connecticut watershed shows very low FWW (watershed-averaged FWW of 15%) for the historic and mid-century periods under both RCPs. There is also little difference between mid-century and late-century for RCP4.5 (watershed-averaged FWW of 17% for RCP4.5 mid-century versus 15% for RCP4.5 late century). By late century there is a substantial difference in FWW between the two RCPs with watershed-averaged FWW remaining low for RCP4.5 (15%) but increasing to 62% for RCP8.5 (Figure 5). In the Upper Connecticut. ARS is very low across all scenarios and time periods (Figure 6). ARS occupies 1% or less of the watershed area for all scenarios and time periods (Figure 7). This implies that in the Upper Connecticut, there is low risk even under severe climate change scenarios of mid-winter snowfall converting to rainfall.

When examining the FWW and ARS projections, it is important to consider that uncertainties and errors/biases in the source datasets influence results. Uncertainties in temperature projections from the NEX-DCP30 downscaled climate data arise from multiple sources, including: (1) short-term deviations from the long-term trends brought about by natural internal variability in the climate system, (2) varying sensitivities to anthropogenic forcing across the suite of global climate models, and (3) the spread among the forcing scenarios (i.e., the different RCPs) (Hawkins & Sutton, 2009). A fourth source of uncertainty is introduced by the spatial downscaling and bias correction of the global climate data. The NEX-DCP30 data inherit any biases that may exist in the monthly PRISM temperatures (Daly et al., 2008) that were used as the training data for bias-correction of the global climate model data (Thrasher et al., 2013). These biases, along with errors introduced by the downscaling method, may be very small relative to the total variability in temperature productions across the ensemble yet they can have a sizable effect on projections of when and where winter temperatures exceed the 0°C threshold (Alder & Hostetler, 2018). The relative importance of the different sources of uncertainty changes with the lead time of the projection. Internal variability in the first couple of decades dominates the spread in projections out to a couple of decades into the future but is replaced by GCM variability and downscaling methodology (in that order) as lead time increases (Alder & Hostetler, 2018). Towards the end of the 21st century, scenario uncertainty becomes the largest source of total uncertainty in future temperatures (Hawkins & Sutton, 2009).

5 | CONCLUSIONS

In this paper we have introduced a suite of snow metrics that can be used individually or in conjunction with existing snow metrics to describe changing snow cover in recent years and for future projections. These new snow metrics are intended to provide a greater understanding of snow's spatial and temporal variability and be relevant to a wide range of researchers and stakeholders. We have produced two globally extensive, retrospective snow metrics: SCF and SDD. These two metrics are readily available and can augment existing station data or provide snow information where none currently exists. The SCF and SDD data that are available through SnowCloudMetrics.app (Crumley et al., 2020) cover the Northern

Hemisphere Water Year and a newly modified version of these metrics allow for highly flexible temporal and spatial subsetting. Users who wish to subset by month for SCF or to produce SDD for the Southern Hemisphere Water Year can download and modify our GEE code for their own use. These remote sensing-derived metrics, currently produced using the MODIS binary snow cover algorithm have the potential for further improvement by instead using fractional snow covered area (Painter et al., 2009; Rittger et al., 2013) or using data from Landsat 8, Sentinel 2 or similar finer resolution sensors.

In addition to the retrospective metrics, we have produced two prospective snow metrics: ARS and FWW. The downscaled climate model output used to create ARS and FWW provide a more physically based approach and 800-m versus 4-km higher spatial resolution compared with the original ARS and FWW of Nolin and Daly (2006).

In applying these four snow metrics to three sample watersheds across the U.S., we have shown that they provide uniquely valuable information that can augment existing SNOTEL data, where such data are available, and provide new snow information in watersheds without snow monitoring networks. Our preliminary assessment suggests that MODIS-derived SCF and SDD are more sensitive to interannual differences in snowpack compared with SNOTEL-derived SCF and SDD. The FWW and ARS metrics are important as prospective climate indicators. Results show that the Truckee watershed in the Sierra Nevada is highly vulnerable to even a slight winter warming whereas the Colorado Headwaters and Upper Connecticut watersheds are colder but increasingly vulnerable by late-century.

As climate models and downscaling methods continue to improve, these prospective metrics will continue to be updated and produced on a global extent, while also offering access and subsetting capabilities through GEE. The emphasis here has been on snow hydrology but these metrics have already demonstrated that they are useful for other applications such as mapping snowline in the Arctic (Verbyla et al., 2017), and wildlife applications in high latitude snowscapes (Boelman et al., 2019; Mahoney et al., 2018; Van De Kerk et al., 2018; Verbyla et al., 2017). In addition to hydrologic application, we believe that there is a global and broad need for snow information, including for winter recreation, wildlife, and snow management for transportation infrastructure.

The snow metrics presented here are simple enough to "tell the story" of snowpack changes over space, are spatially extensive (in some cases, global), are produced in a consistent manner using high-quality data, and are not overly complicated in their interpretation. We anticipate and hope that these snow metrics will serve multiple sectors and stakeholder groups, some of whom have never had access to such information in the past.

ACKNOWLEDGEMENTS

This research was funded by NASA grant #NNX16AG35G, "New Metrics for Snow in a Warming Climate: Indicators for the National Climate Assessment". We thank the two anonymous reviewers for their thoughtful and insightful comments, which greatly improved the paper.

DATA AVAILABILITY STATEMENT

Code and data are publicly available from the following repositories and websites:

SnowCloudMetrics.app is available online www.snowcloudmetrics.app (last accessed 24 May 2021).

GitHub page for SnowCloudMetrics information and scripts is available online at https://github.com/orgs/SnowCloudMetrics (last accessed 24 May 2021).

GitHub page for At-Risk snow and Frequency of a Warm Winter Google Earth Engine scripts is available online at https://github.com/AnneNolin/NewSnowMetrics (last accessed 24 May 2021).

The catalogue of Google Earth Engine datasets is available online at https://developers.google.com/earth-engine/datasets (last accessed 24 May 2021).

ORCID

Anne W. Nolin https://orcid.org/0000-0002-1506-0087
David E. Rupp https://orcid.org/0000-0003-3562-2072
Ryan L. Crumley https://orcid.org/0000-0001-7179-9321
Mariana J. Webb https://orcid.org/0000-0003-0331-2635
Ross T. Palomaki https://orcid.org/0000-0002-3304-9914

REFERENCES

Alder, J. R., & Hostetler, S. W. (2018). The dependence of hydroclimate projections in snow-dominated regions of the Western United States on the choice of statistically downscaled climate data. *Water Resources Research*, *55*(3), 2279–2300. https://doi.org/10.1029/2018WR023458

Boelman, N. T., Liston, G. E., Gurarie, E., Meddens, A. J. H., Mahoney, P. J., Kirchner, P. B., Bohrer, G., Brinkman, T. J., Cosgrove, C. L., Eitel, J. U. H., Hebblewhite, M., Kimball, J. S., LaPoint, S., Nolin, A. W., Pedersen, S. H., Prugh, L. R., Reinking, A. K., & Vierling, L. A. (2019). Integrating snow science and wildlife ecology in Arctic-boreal North America. *Environmental Research Letters*, *14*(1), 010401. https://doi.org/10.1088/1748-9326/aaeec1

Broxton, P., Zeng, X., & Dawson, N. (2019). *Daily 4 km Gridded SWE and Snow Depth from Assimilated In-Situ and Modeled Data over the Conterminous US, Version 1*, Boulder, Colorado USA: NASA National Snow and Ice Data Center Distributed Active Archive Center. https://doi.org/10.5067/0GGPB220EX6A.

Brown, R. D., & Mote, P. W. (2009). The response of northern hemisphere snow cover to a changing climate. *Journal of Climate*, *22*(8), 2124–2145. https://doi.org/10.1175/2008JCLI2665.1

Brown, R. D., & Robinson, D. A. (2011). Northern Hemisphere spring snow cover variability and change over 1922-2010 including an assessment of uncertainty. *The Cryosphere*, *5*(1), 219–229. https://doi.org/10.5194/tc-5-219-2011

Bureau of Reclamation. (in press). Colorado *river basin water supply and demand study*, Update 2020.

Church, J. E. (1935). Principles of snow surveying as applied to forecasting stream flow. *Agricultural Research*, *51*, 97–130.

Cooper, M. G., Nolin, A. W., & Safeeq, M. (2016). Testing the recent snow drought as an analog for climate warming sensitivity of Cascades snowpacks. *Environmental Research Letters*, *11*(8), 084009. https://doi.org/10.1088/1748-9326/11/8/084009

Crumley, R., Nolin, A., Mar, E., & Sproles, E. (2020). SnowCloudMetrics - Snow information for everyone. *Remote Sensing*, *12*, 3341. https://doi.org/10.3390/rs12203341.

Daly, C., Gibson, W. P., Taylor, G. H., & Johnson, G. L. (2002). A knowledge-based approach to the statistical mapping of climate. *Climate Research*, *22*(2), 99–113.

Daly, C., Halbleib, M., Smith, J. I., Gibson, W. P., Doggett, M. K., Taylor, G. H., Curtis, J., & Pasteris, P. P. (2008). Physiographically sensitive mapping of climatological temperature and precipitation across the conterminous United States. *International Journal of Climatology*, *28*, 2031–2064. https://doi.org/10.1002/joc.1688

Dewey, K. F. (1987). Satellite-derived maps of snow cover frequency for the Northern Hemisphere. *Journal of Climate and Applied Meteorology*, *26*, 1210–1229.

Foster, J. L. (1989). The significance of the date of snow disappearance on the arctic tundra as a possible indicator of climate change. *Arctic & Alpine Research*, *21*(1), 60–70. https://doi.org/10.2307/1551517

Foster, J. L., Winchester, J. W., & Dutton, E. G. (1992). The date of snow disappearance on the Arctic tundra as determined from satellite, meteorological station and radiometric in situ observations. *IEEE Transactions on Geoscience and Remote Sensing*, *30*(4), 793–798. https://doi.org/10.1109/36.158874

Frei, A., Robinson, D. A., & Hughes, M. G. (1999). North American snow extent: 1900-1994. *International Journal of Climatology*, *19*(14), 1517–1534. https://doi.org/10.1002/(SICI)1097-0088(19991130)19:14<1517::AID-JOC437>3.0.CO;2-I

Garen, D. (1992). Garen_JWRPM_1992.pdf. *Journal of Water Resources Planning and Management*, *118*(6), 654–670.

Gleason, K. E., Nolin, A. W., & Roth, T. R. (2017). Developing a representative snow-monitoring network in a forested mountain watershed. *Hydrology and Earth System Sciences*, *21*(2), 1137–1147. https://doi.org/10.5194/hess-21-1137-2017

Hammond, J. C., Saavedra, F. A., & Kampf, S. K. (2018a). Global snow zone maps and trends in snow persistence 2001–2016. *International Journal of Climatology*, *38*(12), 4369–4383. https://doi.org/10.1002/joc.5674

Hammond, J. C., Saavedra, F. A., & Kampf, S. K. (2018b). How does snow persistence relate to annual streamflow in mountain watersheds of the Western U.S. with wet maritime and dry continental climates? *Water Resources Research*, *54*(4), 2605–2623. https://doi.org/10.1002/2017WR021899

Harpold, A. A., Dettinger, M., & Rajagopal, S. (2017). Defining snow drought and why it matters. *Eos*, *98*(5), 15–17. https://doi.org/10.1029/2017eo068775

Hawkins, E., & Sutton, R. (2009). The potential to narrow uncertainty in regional climate predictions. *Bulletin of the American Meteorological Society*, *90*(8), 1095–1107. https://doi.org/10.1175/2009BAMS2607.1

Hu, J. M., & Nolin, A. W. (2020). Widespread warming trends in storm temperatures and snowpack fate across the Western United States. *Environmental Research Letters*, *15*(3), 034059. https://doi.org/10.1088/1748-9326/ab763f

Huang, K., Zu, J., Zhang, Y., Cong, N., Liu, Y., & Chen, N. (2018). Impacts of snow cover duration on vegetation spring phenology over the Tibetan Plateau. *Journal of Plant Ecology*, *12*(3), 583–592. https://doi.org/10.1093/jpe/rty051

Karmalkar, A. V., Thibeault, J. M., Bryan, A. M., & Seth, A. (2019). Indentifying credible and diverse GCMs for regional climate change studies—case study: Northeastern United States. *Climatic Change*, *154*(3–4), 367–386. https://doi.org/10.1007/s10584-019-02411-y

Kennedy, K., Lutz, K., Hatfield, C., Martin, L., Barker, T., Kennedy, K., Palmer Richard, N., Detwiler, L., Anleitner, J., & Hickey, J. (2018). *The Connecticut River Flow Restoration Study: A watershed-scale assessment of the potential for flow restoration through dam re-operation*. Northampton, MA.

Knowles, N. (2015). Trends in snow cover and related quantities at weather stations in the conterminous United States. *Journal of Climate*, *19*(8), 4545–4559. https://doi.org/10.1175/JCLI-D-15-0051.1

Lundquist, J. D., Dickerson-Lange, S. E., Lutz, J. A., & Cristea, N. C. (2013). Lower forest density enhances snow retention in regions with warmer winters: A global framework developed from plot-scale observations and modeling. *Water Resources Research*, *49*, 6356–6370. https://doi.org/10.1002/wrcr.20504

Lundquist, J. D., & Lott, F. (2010). Using inexpensive temperature sensors to monitor the duration and heterogeneity of snow-covered areas. *Water Resources Research*, *46*(4), 8–13. https://doi.org/10.1029/2008WR007035

Lynn, E., O'Daly, W., Keeley, F., Dsiwm, D., & Woled, J. (2015). *Perspectives and guidance for climate change analysis*. Available at: https://water.ca.gov/-/media/DWR-Website/Web-Pages/Programs/All-Programs/Climate-Change-Program/Climate-Program-Activities/Files/Reports/Perspectives-Guidance-Climate-Change-Analysis.pdf.

Mahoney, P. J., Liston, G. E., LaPoint, S., Gurarie, E., Mangipane, B., Wells, A. G., Brinkman, T. J., Eitel, J. U. H., Hebblewhite, M., Nolin, A. W., Boelman, N., & Prugh, L. R. (2018). Navigating snowscapes: Scale-dependent responses of mountain sheep to snowpack properties. *Ecological Applications*, *28*(7), 1715–1729. https://doi.org/10.1002/eap.1773

Matson, M., Ropelewski, C. F., & Varnadore, M. S. (1986). *An atlas of satellite-derived northern hemispheric snow cover frequency*. Washington, DC: US Department of Commerce.

McCabe, A. J. J., & Legates, S. R. (1995). Relationships between 700 hPa height anomalies and 1 April snowpack accumulations in the western USA. *International Journal of Climatology*, *14*, 517–530.

Meinshausen, M., Smith, S. J., Calvin, K., Daniel, J. S., Kainuma, M. L. T., Lamarque, J., Matsumoto, K., Montzka, S. A., Raper, S. C. B., Riahi, K., Thomson, A., Velders, G. J. M., & van Vuuren, D. P. P. (2011). The RCP greenhouse gas concentrations and their extensions from 1765 to 2300. *Climatic Change*, *109*(1), 213–241. https://doi.org/10.1007/s10584-011-0156-z

Molotch, N. P., & Bales, R. C. (2006). Comparison of ground-based and airborne snow surface albedo parameterizations in an alpine watershed: Impact on snowpack mass balance. *Water Resources Research*, *42*(5), 1–12. https://doi.org/10.1029/2005WR004522

Montoya, E. L., Dozier, J., Meiring, W., Church, J. E., Hammond, J. C., Saavedra, F. A., & Kampf, S. K. (2014). How does snow persistence relate to annual streamflow in mountain watersheds of the Western U.S. with wet maritime and dry continental climates? *Water Resources Research*, *54*(4), 529. https://doi.org/10.2307/209242

Mote, P., Brekke, L., Duffy, P. B., & Maurer, E. (2011). Guidelines for constructing climate scenarios. *Eos Trans. AGU*, *92*(31), 257. https://doi.org/10.1029/2011EO310001

Mote, P. W. (2003). Trends in snow water equivalent in the Pacific Northwest and their climatic causes. *Geophysical Research Letters*, *30*(12), 1601. https://doi.org/10.1029/2003GL017258

Mote, P. W., Li, S., Lettenmaier, D. P., Xiao, M., & Engel, R. (2018). Dramatic declines in snowpack in the western US. *npj Climate and Atmospheric Science*, *1*(2), 1–6. https://doi.org/10.1038/s41612-018-0012-1

National Operational Hydrologic Remote Sensing Center (2004). *Snow Data Assimilation System (SNODAS) Data Products at NSIDC, Version 1*, Boulder, Colorado USA: National Snow and Ice Data Center (NSIDC). https://doi.org/10.7265/N5TB14TC.

Nolin, A. W. (2012). Perspectives on climate change, mountain hydrology, and water resources in the Oregon Cascades, USA. *Mountain Research and Development*, *32*(S1), S35–S46. https://doi.org/10.1659/MRD-JOURNAL-D-11-00038.S1

Nolin, A. W., & Daly, C. (2006). Mapping 'at risk' snow in the Pacific Northwest. *Journal of Hydrometeorology*, *7*(5), 1164–1171. https://doi.org/10.1175/JHM543.1

Oyler, J. W., Ballantyne, A., Jencso, K., Sweet, M., & Running, S. W. (2015). Creating a topoclimatic daily air temperature dataset for the conterminous United States using homogenized station data and remotely sensed land skin temperature. *International Journal of Climatology*, *35*(9), 2258–2279. https://doi.org/10.1002/joc.4127

Painter, T. H., Rittger, K., McKenzie, C., Slaughter, P., Davis, R. E., & Dozier, J. (2009). Retrieval of subpixel snow covered area, grain size,

and albedo from MODIS. *Remote Sensing of Environment*, *113*(4), 868–879. https://doi.org/10.1016/j.rse.2009.01.001

Painter, T. H., Skiles, S. M., Deems, J. S., Brandt, T. W., & Dozier, J. (2017). Variation in rising limb of Colorado River snowmelt runoff hydrograph controlled by dust radiative forcing snow. *Geophysical Research Letters*, *45*(2), 797–808. https://doi.org/10.1002/2017GL075826

Rittger, K., Painter, T. H., & Dozier, J. (2013). Assessment of methods for mapping snow cover from MODIS. *Advances in Water Resources*, *51*, 367–380. https://doi.org/10.1016/j.advwatres.2012.03.002

Rupp, D. E., Mote, P. W., Bindoff, N. L., Stott, P. A., & Robinson, D. A. (2013). Detection and attribution of observed changes in northern hemisphere spring snow cover. *Journal of Climate*, *26*(18), 6904–6914. https://doi.org/10.1175/JCLI-D-12-00563.1

Serreze, M. C., Clark, M. P., Armstrong, R. L., McGinnis, D. A., & Pulwarty, R. S. (1999). Characteristics of the western United States snowpack from snowpack telemetry (SNOTEL) data. *Water Resources Research*, *35*(7), 2145–2160. https://doi.org/10.1029/1999WR900090

Sproles, E. A., Nolin, A. W., Rittger, K., & Painter, T. H. (2013). Climate change impacts on maritime mountain snowpack in the Oregon Cascades. *Hydrology and Earth System Sciences*, *17*(7), 2581–2597. https://doi.org/10.5194/hess-17-2581-2013

Sproles, E. A., Roth, T. R., & Nolin, A. W. (2017). Future snow? A spatial-probabilistic assessment of the extraordinarily low snowpacks of 2014 and 2015 in the Oregon Cascades. *The Cryosphere*, *11*(1), 331–341. https://doi.org/10.5194/tc-11-331-2017

Sproles, E. A., Crumley, R., Nolin, A., Mar, E., & Lopez Moreno, J. (2018). Snowcloudhydro—A new framework for forecasting streamflow in snowy, data-scarce regions. *Remote Sensing*, *10*(8), 1276. https://doi.org/10.3390/rs10081276.

Sterle, K., Hatchett, B. J., Singletary, L., & Pohll, G. (2019). Hydroclimate variability in snow-fed river systems: Local water managers' perspectives on adapting to the new normal. *Bulletin of the American Meteorological Society*, *100*(6), 1031–1048. https://doi.org/10.1175/BAMS-D-18-0031.1

Sturm, M., Holmgren, J., & Liston, G. (1995). A seasonal snow cover classification system for local to global applications. *Journal of Climate*, *8*(5), 1261–1283.

Thomson, A. M., Calvin, K. V., Smith, S. J., Kyle, G. P., Volke, A., Patel, P., Delgado-Arias, S., Bond-Lamberty, B., Wise, M. A., Clarke, L. E., & Edmonds, J. A. (2011). RCP4.5: A pathway for stabilization of radiative forcing by 2100. *Climatic Change*, *109*(1), 77–94. https://doi.org/10.1007/s10584-011-0151-4

Thrasher, B., Xiong, J., Wong, W., Melton, F., Michaelis, A., & Nemani, R. (2013). Downscaled climate projections suitable for resource management. *Eos, Transactions American Geophysical Union*, *94*(37), 321–323.

Van De Kerk, M., Verbyla, D., Nolin, A. W., Sivy, K. J., & Prugh, L. R. (2018). Range-wide variation in the effect of spring snow phenology on Dall sheep population dynamics. *Environmental Research Letters*, *13*(7), 075008. https://doi.org/10.1088/1748-9326/aace64

Verbyla, D., Hegel, T., Nolin, A. W., van de Kerk, M., Kurkowski, T. A., & Prugh, L. R. (2017). Remote sensing of 2000-2016 alpine spring snowline elevation in dall sheep mountain ranges of Alaska and Western Canada. *Remote Sensing*, *9*(11), 1157. https://doi.org/10.3390/rs9111157

Wayand, N. E., Marsh, C. B., Shea, J. M., & Pomeroy, J. W. (2018). Globally scalable alpine snow metrics. *Remote Sensing of Environment*, *213*, 61–72. https://doi.org/10.1016/j.rse.2018.05.012

Westerling, A. L., Hidalgo, H. G., Cayan, D. R., & Swetnam, T. W. (2006). Warming and earlier spring increase Western U.S. Forest wildfire activity. *Science*, *313*(5789), 940–943. https://doi.org/10.1126/science.1128834

Xiao, X., Zhang, Q., Boles, S., Rawlins, M., & Moore, I. (2004). Mapping snow cover in the pan-Arctic zone, using multi-year (1998-2001) images from optical VEGETATION sensor. *International Journal of Remote Sensing*, *25*(24), 5731–5744. https://doi.org/10.1080/01431160410001719867

Xie, J., Jonas, T., Rixen, C., de Jong, R., Garonna, I., Notarnicola, C., Asam, S., Schaepman, M. E., & Kneubühler, M. (2020). Land surface phenology and greenness in Alpine grasslands driven by seasonal snow and meteorological factors. *Science of the Total Environment*, *725*, 138380. https://doi.org/10.1016/j.scitotenv.2020.138380

How to cite this article: Nolin, A. W., Sproles, E. A., Rupp, D. E., Crumley, R. L., Webb, M. J., Palomaki, R. T., & Mar, E. (2021). New snow metrics for a warming world. *Hydrological Processes*, *35*(6), e14262. https://doi.org/10.1002/hyp.14262